

**PHARMACOLOGICAL POTENTIAL OF  
*MORINGA OLEIFERA* SILVER NANOPARTICLES  
TARGETING ANGIOGENESIS AND  
COLORECTAL CANCER CELL LINES  
INHIBITION**

**ROLLA ZIYAD MUSTAFA AL-SHALABI**

**UNIVERSITI SAINS MALAYSIA**

**2025**

**PHARMACOLOGICAL POTENTIAL OF  
*MORINGA OLEIFERA* SILVER NANOPARTICLES  
TARGETING ANGIOGENESIS AND  
COLORECTAL CANCER CELL LINES  
INHIBITION**

by

**ROLLA ZIYAD MUSTAFA AL-SHALABI**

**Thesis submitted in fulfilment of the requirements  
for the degree of  
Doctor of Philosophy**

**August 2025**

## ACKNOWLEDGEMENT

بِسْمِ اللَّهِ الرَّحْمَنِ الرَّحِيمِ  
وَفَوْقَ كُلِّ ذِي عِلْمٍ عَلِيمٌ

All praise is to Allah, the Most Gracious and the Most Merciful, for giving me the power and strength to complete my study.

Firstly, I would like to thank my honourable supervisor, Dr Nozlana Binti Abdul Samad (Advanced Medical and Dental Institute, USM), for her continuous care, kindness, and knowledge, as well as her dedication to standing by my side inspired me through my study. I am grateful to Dr Ibrahim Al Deeb (Al Zarqa University, Jordan) for his continuous guidance, significant contributions to my research, and helped me achieve my dream after years of struggle. I would also like to thank my distinguished co-supervisor, Dr Lim Vuanghao (Advanced Medical and Dental Institute, USM), for his significant input, guidance, and knowledge that he has shared with me. I would like to express my sincere gratitude to Dr Ayesha Fatima for her invaluable guidance, support, and insightful contributions to this research. I extend my appreciation to thank Julia Joseph and Melissa Kilus for her contributions throughout my journey. My heartfelt gratitude goes to all my friends who had supported me. No words can express my feelings to them, and I shall never forget your kind words and generous support, which have strongly impacted me and my behaviour.

Finally, I owe my greatest thankfulness and appreciation to my husband (Loay), my children (Mohammad, Ahmad, Mahmoud, Sara, and Abdulrahman), my father (Ziyad), and my mother-in-law (Shahnaz) for their invaluable and endless inspiration and prayers in supporting me to be successful in life.

## TABLE OF CONTENTS

<b>ACKNOWLEDGEMENT</b> .....	<b>ii</b>
<b>TABLE OF CONTENTS</b> .....	<b>iii</b>
<b>LIST OF TABLES</b> .....	<b>xi</b>
<b>LIST OF FIGURES</b> .....	<b>xiii</b>
<b>LIST OF SYMBOLS</b> .....	<b>xxi</b>
<b>LIST OF UNITS</b> .....	<b>xxii</b>
<b>LIST OF ABBREVIATIONS</b> .....	<b>xxiii</b>
<b>LIST OF APPENDICES</b> .....	<b>xxvii</b>
<b>ABSTRAK</b> .....	<b>xxviii</b>
<b>ABSTRACT</b> .....	<b>xxx</b>
<b>CHAPTER 1 INTRODUCTION</b> .....	<b>1</b>
1.1 Research Background .....	1
1.2 Angiogenesis.....	2
1.3 Silver Nanoparticles.....	4
1.4 <i>Moringa oleifera</i> .....	5
1.5 Problem Statement .....	6
1.6 Objective of the Study .....	7
1.6.1 Main Objective .....	7
1.6.2 Specific Objective.....	8
1.7 Research Questions .....	8
1.8 Research Hypothesis .....	9
<b>CHAPTER 2 LITERATURE REVIEW</b> .....	<b>10</b>
2.1 Introduction to Cancer and Its Therapy .....	10
2.1.1 Mechanisms of Tumour Growth and Metastasis .....	11
2.1.2 Conventional Approaches to Cancer Treatment .....	11

2.1.3	Innovative Cancer Therapies .....	12
2.2	Colorectal Cancer.....	12
2.2.1	Pathogenic Mechanisms in Colon Cancer Development .....	14
2.2.2	Treatment Modalities for Colorectal Cancer .....	14
2.2.3	Novel Therapeutic Approaches for Colorectal Cancer .....	16
2.3	Angiogenesis: A Crucial Process in Cancer Progression.....	16
2.3.1	The Role of Anti-Angiogenic Therapy in Tumour Development and Metastasis.....	18
2.3.2	Comprehensive Anti-Angiogenic Therapies and Their Applications in Cancer Treatment .....	22
2.3.2(a)	Optimizing Anti-Angiogenic Therapy Through Combination Approaches .....	23
2.3.2(b)	Adjuvant Anti-Angiogenic Strategies in Cancer Management .....	24
2.3.2(c)	Natural Compounds with Anti-Angiogenic Properties.....	25
2.4	Essential Proteins in Tumour-Induced Angiogenesis.....	26
2.4.1	Vascular Endothelial Growth Factor.....	27
2.4.2	Angiogenin .....	27
2.4.3	Angiopoietins.....	28
2.4.4	Monocyte Chemoattractant Protein-1 .....	29
2.4.5	Tissue Inhibitors of Metalloproteinase .....	29
2.4.6	The Role of IL-8 and Other Pro-Inflammatory Cytokines in Angiogenesis Promotion.....	30
2.5	Angiotherapy Using Natural Products .....	31
2.6	<i>M. oleifera</i> and Its Bioactive Potential in Anti-Angiogenic Treatments.....	32
2.6.1	Phytochemicals in <i>M. oleifera</i> Leaves.....	35
2.6.2	Targeting Angiogenic Pathways and Anti-Cancer Properties of <i>M. oleifera</i> .....	37
2.7	Extraction and Isolation Techniques for Bioactive Compounds from <i>M.</i> <i>oleifera</i> .....	38

2.8	Green Synthesis of Nanoparticles Using Plant Extracts .....	40
2.8.1	Environmental and Biomedical Advantages.....	42
2.8.2	Investigation of Plant Extracts in Green Silver Nanoparticles Synthesis.....	43
2.8.3	The Role of Phytochemicals in Nanoparticle Mechanisms and Benefits of Biological Methods Compared to Chemical Approaches .....	45
2.8.3(a)	Mechanisms of Reduction .....	45
2.8.3(b)	Mechanisms of Stabilization .....	46
2.8.3(c)	Advantages of Biological Methods over Chemical Synthesis.....	46
2.9	Techniques for the Characterization and Analysis of Nanoparticles .....	48
2.9.1	Ultraviolet–Visible Spectroscopy (UV-Vis Spectroscopy).....	48
2.9.2	Dynamic Light Scattering (DLS) .....	49
2.9.3	High-Performance Liquid Chromatography coupled with Tandem Mass Spectrometry (HPLC-MS/MS) .....	49
2.10	Nanoparticles in Cancer Treatment: Mechanisms and Applications .....	50
2.10.1	Nanoparticles As Drug Delivery Systems In Cancer Therapy .....	50
2.11	Cellular Assays for Evaluating the Efficacy of Nanoparticles.....	51
2.11.1	Proliferation Assay .....	52
2.11.1(a)	MTT Assay .....	52
2.11.1(b)	Colony Formation Assay .....	53
2.11.2	Techniques for Evaluating Endothelial Cells Following Nanoparticle Treatment .....	54
2.11.2(a)	Cell Morphology .....	54
2.11.2(b)	Migration Assay .....	56
2.11.2(c)	Invasion Assay.....	56
2.11.2(d)	Tube Formation Assay.....	57
2.11.3	The Role of Endothelial Cells in Angiogenesis and The Effects of Nanoparticles.....	58

2.12	Advanced Assays in Angiogenesis Evaluation .....	59
2.12.1	3D Spheroid Assay .....	59
2.12.2	Chorioallantoic Membrane Assay .....	60
2.13	Protein Expression Analysis and Molecular Docking Studies.....	61
2.13.1	Assessment Techniques: RayBiotech Protein Arrays versus Western Blot .....	61
2.13.2	Molecular Docking and Its Nanoparticles Related Applications .....	62
<b>CHAPTER 3 RESEARCH METHODOLOGY.....</b>		<b>64</b>
3.1	Materials .....	64
3.1.1	Chemicals and Reagents .....	64
3.1.2	Instruments and Equipment .....	65
3.2	Methodology .....	66
3.2.1	Study Design.....	66
3.2.2	<i>Moringa oleifera</i> Leaves Collection.....	67
3.2.3	Sequential Extract Preparation of <i>M. oleifera</i> Leaves.....	68
3.2.4	Nanoparticle Synthesis from the Water-Soluble Extract .....	68
3.2.4(a)	Analysis and Characterisation of <i>M. oleifera</i> Leaf Extract and AgNPs .....	69
3.2.4(a)(i)	UV- Visible Spectrometry .....	69
3.2.4(a)(ii)	Dynamic Light Scattering Analysis .....	69
3.2.4(a)(iii)	HPLC-MS/MS QTOF Analysis .....	70
3.2.5	Proliferative Assay.....	70
3.2.5(a)	Maintenance and Culturing of Cell Lines .....	71
3.2.5(a)(i)	Cell Lines and Medium Conditions .....	71
3.2.5(a)(ii)	Cell Culture and Daily Monitoring of Cells .....	71
3.2.5(a)(iii)	Sub-culturing and Cell Counting .....	71
3.2.5(a)(iv)	Cryopreservation of Cell Lines.....	73

3.2.5(b)	MTT Assay for Growth Inhibition of Colorectal Cancer Cell Line.....	73
3.2.6	Cell Morphology Assay .....	75
3.2.7	Endothelial Cellular Migration Assay .....	75
3.2.8	Colony Formation Assay on Endothelial Cell Line.....	76
3.2.9	Assessment of Endothelial Cell Invasion .....	77
3.2.10	Endothelial Cell Tube Formation Assay .....	78
3.2.11	Ex Vivo Anti-Angiogenic Evaluation of MO-AgNPs Using Rat Aortic Ring Assay.....	79
3.2.11(a)	Experimental Animals .....	79
3.2.11(b)	Culturing Rat Aortic Rings.....	79
3.2.11(c)	Culture Medium .....	80
3.2.11(d)	Rat Aortic Rings Treatment.....	80
3.2.11(e)	Quantification and Evaluation of Neovascularisation .....	80
3.2.12	Hanging Drop Spheroids Model for Co-Culturing EA.hy926 and HT29 Cells.....	81
3.2.12(a)	Formation of Spheroid.....	81
3.2.12(b)	Treatment of Spheroids with MO-AgNPs.....	83
3.2.13	Chorioallantoic Membrane (CAM) Assay.....	83
3.2.14	Effect of MO-AgNPs on the Protein Expression of Treated EA.hy926 Cells Using Protein Array .....	84
3.2.14(a)	Assay for Human Angiogenesis Antibody Array .....	85
3.2.14(b)	Preparation of Samples.....	88
3.2.14(c)	Sample Incubation with RayBio Human Angiogenesis Antibody Array .....	88
3.2.14(d)	Fluorescent Signal Intensity Analysis .....	89
3.2.14(e)	Data Interpretation.....	89
3.2.15	Molecular Docking of the Major Compounds in MO-AgNPs Against Anti-angiogenic Targets .....	90

3.2.15(a)	Development of the Ag <sub>3</sub> Clusters .....	90
3.2.15(b)	Conjugating the Compounds with Ag <sub>3</sub> .....	91
3.2.15(c)	Molecular Docking.....	93
3.2.15(c)(i)	Protein Preparation .....	93
3.2.15(c)(ii)	Docking Studies Simulations.....	93
3.2.16	Statistical Analysis.....	94
<b>CHAPTER 4 RESULTS .....</b>		<b>95</b>
4.1	<i>M. oleifera</i> Leaf Collection.....	95
4.2	Sequential Extract Preparation of <i>M. oleifera</i> Leaves .....	95
4.3	Synthesis of MO-AgNPs using the Water-Soluble Extract.....	96
4.4	Analysis and Characterisation of <i>M. oleifera</i> Leaf Extract and MO-AgNPs .....	97
4.4.1	Percentage Yield .....	97
4.4.2	UV-Vis Spectrometry.....	97
4.4.3	Dynamic Light Scattering Analysis.....	98
4.4.4	Identification of Major Compounds in MO-AgNPs using HPLC-MS/MS QTOF Analysis.....	100
4.5	Cell Viability and Anti-Proliferative Effect .....	102
4.6	Cell Morphology Assay .....	106
4.7	Endothelial Cell Migration Assay .....	107
4.8	Cytotoxic Properties of MO-AgNPs Towards EA.hy926 Cells Using Colony Assay .....	110
4.9	In Vitro EA.hy926 Invasion Inhibition by MO-AgNPs.....	112
4.10	Endothelial Tube Formation Inhibition by MO-AgNPs .....	115
4.11	Neovascularisation Formation Inhibition of MO-AgNPs Using Ex Vivo Rat Aortic Ring Assay.....	117
4.12	Anti-Tumour Properties of MO-AgNPs Using Co-Cultured 3D Spheroid Model .....	118
4.13	Effects of MO-AgNPs on the Angiogenesis Mechanistic Pathway Using CAM Assay .....	122

4.14	Human Angiogenesis Antibody Protein Array-Based Identification of the Molecular Targets of MO-AgNPs on EC Lines .....	125
4.15	Docking Study for the Major Compounds of MO-AgNPs Against Anti-angiogenic Targets .....	128
4.15.1	The Binding Site of Each Ligand with Several Proteins .....	128
4.15.1(a)	4-p-coumaroylquinic acid-Ag <sub>3</sub> .....	128
4.15.1(b)	2,4-dichlorobenzoate-Ag <sub>3</sub> .....	131
4.15.1(c)	5-methyl-octanoic acid-Ag <sub>3</sub> .....	133
4.15.1(d)	R-pantolactone-Ag <sub>3</sub> .....	135
4.16	Anti-angiogenesis Effects of Active Compounds (4-p-coumaroylquinic acid) in MO-AgNPs using the CAM Assay .....	140
<b>CHAPTER 5 DISCUSSION.....</b>		<b>143</b>
5.1	Preparation, Synthesis, and Characterisation of Plant Extract Samples .....	143
5.1.1	MO-AgNPs Synthesis and UV-Vis Spectroscopy .....	143
5.1.2	Characterisation of MO-AgNPs Using Dynamic Light Scattering .....	145
5.1.3	Identification of MO-AgNPs Phytochemical Compounds .....	146
5.2	In Vitro Anti-Angiogenic Effects of MO-AgNPs Against EA.hy926 Cells .....	148
5.2.1	Anti-Proliferative of MO-AgNPs Towards EA.hy926 Cells .....	148
5.2.2	Clonogenic Assay of MO-AgNPs Towards EA.hy926 Cells .....	150
5.2.3	Morphological Assessment of MO-AgNPs treated EA.hy926 .....	152
5.2.4	Anti-Migration Characteristics of MO-AgNPs Towards EA.hy926 Cells .....	153
5.2.5	Inhibition of EA.hy926 Cell Invasion by MO-AgNPs .....	154
5.2.6	Inhibition of Endothelial Tube Formation by MO-AgNPs .....	155
5.3	Ex Vivo Anti-Angiogenic Evaluation of MO-AgNPs Using Rat Aortic Ring Assay .....	157
5.4	Simulated In Vivo Models for Assessing of MO-AgNPs Therapeutic Efficacy .....	159

5.4.1	Tumour Growth Inhibition after MO-AgNPs Treatment using the Co-Cultured 3D Spheroid Model.....	159
5.4.2	Chorioallantoic Membrane Assay Effects of MO-AgNPs via the Angiogenesis Mechanistic Pathway .....	160
5.5	Anti-angiogenic Mechanism of MO-AgNPs Towards EA.hy926 Cells .....	162
5.5.1	Human Angiogenesis Antibody Protein Array-Based Identification of the Molecular Targets of MO-AgNPs on EA.hy926.....	162
5.5.2	Docking Study for Assessing the Major compounds of MO-AgNPs Against Anti-angiogenic Targets .....	169
5.6	Confirmation of the Anti-angiogenesis Effect of MO-AgNPs Active Compound 4-p-coumaroylquinic acid using the CAM Assay .....	170
<b>CHAPTER 6 CONCLUSION .....</b>		<b>173</b>
6.1	Conclusion .....	173
6.2	Study Limitation .....	175
6.3	Future Recommendations .....	175
<b>REFERENCES.....</b>		<b>177</b>
<b>APPENDICES</b>		
<b>LIST OF PUBLICATIONS</b>		

## LIST OF TABLES

	<b>Page</b>
Table 2.1	Summary of some natural plants with anti-angiogenic effects. .... 32
Table 2.2	Taxonomic classification of <i>M. oleifera</i> . .... 33
Table 2.3	Traditional uses of <i>M. oleifera</i> . .... 34
Table 2.4	Key bioactive compounds found in <i>M. oleifera</i> with their therapeutic effects. .... 36
Table 2.5	Highlights a range of solvents utilized in various extraction methods for <i>M. oleifera</i> in previous studies. .... 40
Table 2.6	Summary of nanoparticles, their biological activities, shapes, and sizes. .... 42
Table 2.7	Advantages and disadvantages of chemical, biological, and physical approaches for nanoparticle synthesis ..... 48
Table 3.1	List the chemicals and reagents used in this study. .... 64
Table 3.2	The instrument and equipment employed in this study. .... 65
Table 3.3	Targeted angiogenic factors that were investigated using the RayBio human angiogenesis antibody array (RayBiotech Inc., USA). This array detects the expression levels of these targets by measuring signal intensities. .... 85
Table 3.4	Bond lengths and angle values between the Ag atoms in the Ag <sub>3</sub> clusters, D <sub>3h</sub> and C <sub>2v</sub> , and Ag <sub>3</sub> conjugates. .... 91
Table 3.5	Proteins utilised in the molecular docking study, with their corresponding PDB IDs and binding sites coordinates. .... 93
Table 4.1	List of compounds detected in <i>M. oleifera</i> aqueous extracts (MO1) and (MO2) using HPLC-MS/MS analysis. .... 101
Table 4.2	Closure percentage of EA.hy926 cells at different MO-AgNP concentrations. .... 108
Table 4.3	Colony formation assay of EA.hy926 cells at different MO-AgNP concentrations. .... 111
Table 4.4	Percentage inhibition of neovascularisation after treatment with 12, 6, 3, and 1.5 µg/mL of MO-AgNPs using the rat aortic ring assay. .... 118

Table 4.5	Size percentage of co-cultured spheroids compared to the size of the untreated group (0.05% DMSO and 0.05% deionised water). The results are expressed as the mean $\pm$ SD. *P $\leq$ 0.05, **P $\leq$ 0.01 (Kruskal-Wallis test). ....	119
Table 4.6	The signal intensity and fold change of the angiogenic factors in the supernatant of untreated sample (0.05% DMSO and 0.05% deionised water) and treated sample (12 $\mu$ g/mL of MO-AgNPs). ...	126
Table 4.7	Estimated free binding energy of the main compounds in MO-AgNPs with angiogenic factors using AutoDock Tools 1.5.7.....	139
Table 5.1	Summarizes the function of each protein related to angiogenesis and the effect of MO-AgNPs based on our findings.....	166

## LIST OF FIGURES

	<b>Page</b>
Figure 1.1	The role of sprouting angiogenesis in tumour development. (A) During the early stages of growth, the tumour is very small and depends on existing blood arteries for oxygen and nutrients. (B) As the tumour expands, new vessels sprout from local existing blood vessels to meet the increased demand for oxygen and nutrients. (C) Sprouting angiogenesis creates a more complicated structure of vascular to ensure enough blood supply to the expanding tumour (Haibe et al., 2020). ..... 3
Figure 2.1	The angiogenesis process comprises multiple stages: vessel activation, followed by pericyte detachment, EC migration, and sprout formation that connects to create new microvascular networks supported by a basement membrane (Laschke, Gu and Menger, 2022). ..... 18
Figure 2.2	Angiogenesis involves the formation of blood vessels, rendering it a critical role in the growth and metastasis of solid cancers. Various factors, such as low oxygen levels, inflammation, and growth signals, can trigger cancer cells to secrete substances that promote the development of blood vessels in tumour cells, consequently aiding their progression (Ayoub et al., 2022)..... 21
Figure 2.3	Green synthesis of nanoparticles. Metal ions undergoes reduction, leading to the formation of nanoparticles with the assistance of natural reducing agents derived from plants, fungi, bacteria or viruses. Notably, an increase in temperature accelerates the reaction time, enhancing the overall production of nanoparticles. This figure was created using Biorender.com. .... 41
Figure 2.4	Schematic representation of the green synthesis of silver nanoparticles (AgNPs) using AgNO <sub>3</sub> and plant extracts, which act as reducing, stabilizing, and capping agents. Bioactive compounds in the plant extracts facilitate the reduction of silver ions (Ag <sup>+</sup> ) to silver nanoparticles (Ag <sup>0</sup> ). This figure was created using Biorender.com ..... 45
Figure 3.1	Flow chart illustrating the overall study design. .... 67
Figure 3.2	The grid outline of a glass hemocytometer highlights four groups of 16 squares designated for counting, marked by blue boxes labeled a, b, c, and d. .... 73
Figure 3.3	Formation of spheroid for the spheroid assay on the inner surface of 6-well plates, creating 3D tumour-like structures for spheroid assays to evaluate the anti-angiogenic effects of MO-AgNPs. .... 82

Figure 3.4	The 43 targeted angiogenic factors were fixed on two slides: 20 targets on slide 1 and 23 on slide 2. POS: Positive control (contains equal amounts of biotinylated IgGs). NEG: Negative control (a protein-containing buffer). RayBio human Angiogenesis Antibody Array G-Series 1000.....	86
Figure 3.5	Working principle of the RayBio human angiogenesis array (RayBio user manual, P.7). After sample addition, a biotin-conjugated anti-cytokine mixture is added to the wells, followed by streptavidin-fluor, allowing for the detection of angiogenic markers, signal capture, and data analysis. ....	87
Figure 3.6	The optimised Ag <sub>3</sub> clusters in the (a) D <sub>3h</sub> symmetry and (b) C <sub>2v</sub> symmetry. ....	90
Figure 3.7	The optimised (a) 4-p-coumaroylquinic acid-Ag <sub>3</sub> , (b) 2,4-dichlorobenzoate-Ag <sub>3</sub> , (c) 5-methyl-octanoic acid-Ag <sub>3</sub> , and (d) R-pantolactone-Ag <sub>3</sub> .....	92
Figure 4.1	Appearance of <i>M. oleifera</i> : (a) Fresh stem and leaves; (b) Dried leaves; (c) Ground and sieved leaf powder; (d) Ethanol extract; (e) 50% Ethanol extract; (f) Aqueous extract.....	96
Figure 4.2	Formation of black colour indicating the synthesis of <i>M. oleifera</i> silver nanoparticles (MO-AgNPs). Aqueous extract of <i>M. oleifera</i> and 1 mM silver nitrate (AgNO <sub>3</sub> ) were incubated in a water bath at 60°C with agitation for 8 hours; (a) Aqueous extract; (b) MO-AgNPs. ....	97
Figure 4.3	UV-Vis spectrometry of MO-AgNPs with a distinct band at 430 nm. The impact of incubation time on MO-AgNPs formation was analyzed using UV-Vis spectrometry. ....	98
Figure 4.4	Size distribution intensity of MO-AgNPs in three trials. The particle size distribution of MO-AgNPs was determined using dynamic light scattering. ....	99
Figure 4.5	Zeta potential distribution of MO-AgNPs. The Zeta potential of MO-AgNPs was measured at room temperature using a Malvern Nano Zetasizer. ....	100
Figure 4.6	Proposed reaction mechanism of the main compounds (4-p-coumaroylquinic acid ) in <i>M. oleifera</i> with AgNPs for forming MO-AgNPs. The process involves the reduction of silver ions (Ag <sup>+</sup> ) to metallic silver (Ag <sup>0</sup> ), facilitated by the bioactive compound 4-p-coumaroylquinic acid, leading to the formation of stable silver nanoparticles. ....	102
Figure 4.7	Cell viability of the HT29 cell line after incubation with various concentrations of (a) MO-AgNP and (b) ethanolic extract of <i>M. oleifera</i> after 72 hrs. The cell viability was evaluated using MTT	

	assay. Each data point represents the mean $\pm$ standard deviation of results from independent experiments. ....	104
Figure 4.8	The cell viability of EA.hy926 cell line after 72 hrs of incubation with various concentrations of (a) MO-AgNP and (b) ethanolic extract of <i>M. oleifera</i> . Each data point represents the mean $\pm$ standard deviation of results from independent experiments.....	104
Figure 4.9	Comparison of cell viability of (a) EA.hy926 and (b) HT29 cell lines after 72 hrs of incubation with various concentrations of MO-AgNPs and ethanolic extract of <i>M. oleifera</i> . Each data point represents the mean $\pm$ standard deviation of results from independent experiments. All data points show statistical significance ( $P \leq 0.05$ ) except 12.5 $\mu\text{g/mL}$ of MO-AgNPs. For the ethanolic extract of <i>M. oleifera</i> , statistical significance ( $P \leq 0.05$ ) was only observed at 100 and 200 $\mu\text{g/mL}$ concentrations. ....	105
Figure 4.10	Comparison of $\text{IC}_{50}$ of MO-AgNPs against EA.hy926 and HT29 cell lines at 24, 48, and 72 hrs. The $\text{IC}_{50}$ values are presented above the respective bar charts. Each data point represents the mean $\pm$ standard deviation of results from independent experiments. Statistical significance ( $*P \leq 0.05$ ) indicates differences between the two cell lines at the same time point, as determined by the Kruskal–Wallis test. A lower $\text{IC}_{50}$ value reflects higher cytotoxic potency of MO-AgNPs. ....	106
Figure 4.11	Cell morphology of EA.hy926 ( $5 \times 10^5$ cells) before and after treatment with $\text{IC}_{50}$ of MO-AgNPs for 72 hrs, using an inverted microscope at $200\times$ magnification. ....	107
Figure 4.12	Closure percentage of EA.hy926 cells treated with varying concentrations of MO-AgNPs after 24 hrs compared to the negative control. Results are expressed as the mean $\pm$ SD from independent experiments. Statistical significance compared to the negative control; $*P \leq 0.05$ (* at 6 $\mu\text{g/mL}$ ), $**P \leq 0.01$ (** at 12 $\mu\text{g/mL}$ ) (Kruskal–Wallis test). ....	108
Figure 4.13	Migration of EA.hy926 cells at different concentrations of MO-AgNPs at 0 and 24 hrs. Images were captured using an inverted microscope at $40\times$ magnification. The negative control consists of 0.05% DMSO and 0.05% deionised water. (Scale; 20 $\mu\text{m}$ ). ....	109
Figure 4.14	Percentage inhibition of EA.hy926 cell migration at different concentrations after 24 hrs. The results are expressed as the mean $\pm$ SD of independent experiments. Statistical significance compared to the negative control; $*P \leq 0.05$ (* at 6 $\mu\text{g/mL}$ ), $**P \leq 0.01$ (** at 12 $\mu\text{g/mL}$ ) (Kruskal–Wallis test). ....	110
Figure 4.15	Colony formation assay depicting the surviving fraction (SF%) of EA.hy926 colonies after 72 hrs of exposure to MO-AgNPs at varying concentrations. The results are expressed as the mean $\pm$	

	SD of independent experiments. Statistical significance compared to the negative control; * $P \leq 0.05$ (* at 6 $\mu\text{g/mL}$ ), ** $P \leq 0.01$ (** at 12 $\mu\text{g/mL}$ ) (Kruskal–Wallis test).....	111
Figure 4.16	EA.hy926 colonies in each well after 72 hrs of exposure to a) 0.05% DMSO and 0.05% deionised water (negative control), b) 1.5 $\mu\text{g/mL}$ of MO-AgNPs, c) 3 $\mu\text{g/mL}$ of MO-AgNPs, d) 6 $\mu\text{g/mL}$ of MO-AgNPs, and e) 12 $\mu\text{g/mL}$ of MO-AgNPs. The SF was $71.9 \pm 2.5\%$ , $58.0 \pm 1.5\%$ , $50.7 \pm 0.5\%$ , and $48.5 \pm 0.5\%$ , respectively.....	111
Figure 4.17	MO-AgNPs significantly inhibited the invasion of EA.hy926 cells after 24 hrs of treatment with 12, 6, 3, and 1.5 $\mu\text{g/mL}$ of MO-AgNPs, 50 $\mu\text{M}$ quercetin (positive control), and 0.05% DMSO and 0.05% deionised water (negative control). Images were captured using an inverted microscope at 40 $\times$ magnification. ....	113
Figure 4.18	Number of EA.hy926 cells that invaded the Matrigel/ $\text{mm}^2$ after 24 hrs of treatment with 12, 6, 3, and 1.5 $\mu\text{g/mL}$ of MO-AgNPs, 50 $\mu\text{M}$ quercetin (positive control), and 0.05% DMSO and 0.05% deionised water (negative control). The results are expressed as the mean $\pm$ SD of independent experiments. Statistical significance compared to the negative control; * $P \leq 0.05$ , ** $P \leq 0.01$ (Kruskal–Wallis test).....	114
Figure 4.19	Percentage inhibition of EA.hy926 cell invasion by MO-AgNPs or quercetin (positive control) when normalised with the negative control. The results are expressed as the mean $\pm$ SD of independent experiments. Statistical significance compared to the negative control; * $P \leq 0.05$ (* at 6 $\mu\text{g/mL}$ ), ** $P \leq 0.01$ (** at 12 $\mu\text{g/mL}$ and positive control) (Kruskal–Wallis test).....	114
Figure 4.20	Treatment with MO-AgNPs at all concentrations resulted in nearly 100% inhibition of tube formation by EA.hy926 cells, compared to the positive control (quercetin, 50 $\mu\text{M}$ ), when normalized against the untreated cells (0.05% DMSO and 0.05% deionized water) after 2.5 hours of incubation. No enclosed or tubular structures were observed in any of the MO-AgNP-treated groups during this period. In contrast, untreated EA.hy926 cells formed visible tube-like networks. Images were captured using an inverted microscope at 40 $\times$ magnification. ....	116
Figure 4.21	Inhibition of neovascularisation formation after 7 days of treatment with [(a) Negative control (0.05% DMSO and 0.05% deionised water); (b) 100 $\mu\text{g/mL}$ suramin; (c) 12 $\mu\text{g/mL}$ of MO-AgNPs; (d) 6 $\mu\text{g/mL}$ of MO-AgNPs; (e) 3 $\mu\text{g/mL}$ of MO-AgNPs, and (f) 1.5 $\mu\text{g/mL}$ of MO-AgNPs]. The highest percentage inhibition was recorded using 12 $\mu\text{g/mL}$ of MO-AgNPs at $83.8 \pm 0.081\%$ ( $P \leq 0.05$ ). Red arrow indicates blood vessel. Images	

	were captured using an inverted microscope at 40× magnification. ....	117
Figure 4.22	Percentage of neovascularization formation inhibition of MO-AgNPs at different concentrations based on the rat aortic ring assay. The results are expressed as the mean ± SD of independent experiments. Statistical significance compared to the negative control; *P ≤ 0.05 (* at positive control), **P ≤ 0.01 (** at 12 and 6 µg/mL) (Kruskal–Wallis test).....	118
Figure 4.23	Co-culture spheroid growth from day 0 to day 14. The spheroid was composed of HT29 and EA.hy926 cell lines. A significant growth inhibition was recorded after treatment with (1.5, 3, 6, and 12) µg/mL of MO-AgNPs and 50 µM quercetin (positive control) at day 14. Images were captured using an inverted microscope at 40× magnification.....	120
Figure 4.24	Size percentage of the co-cultured spheroid between the treated and untreated groups. The treated groups were exposed to 12, 6, 3, and 1.5 µg/mL of MO-AgNPs, while the positive control was treated with 50 µM quercetin (positive control). The results are measured at 0, 3, 8, and 14 days. The size of the spheroid was statistically significant at day 14 after treatment with 6 µg/mL and 12 µg/mL of MO-AgNPs and 50 µM quercetin. *P ≤ 0.05, **P ≤ 0.01 (Kruskal-Wallis test).....	121
Figure 4.25	Percentage inhibition of co-cultured spheroids after 14 days of exposure to 12, 6, 3, and 1.5 µg/mL of MO-AgNPs and 50 µM quercetin (positive control). Inhibition% of the spheroid was statistically significant at day 14 after treatment with 6 µg/mL and 12 µg/mL of MO-AgNPs and 50 µM quercetin. *P ≤ 0.05, **P ≤ 0.01 (Kruskal-Wallis test).....	121
Figure 4.26	Varying appearances of CAM before and after treatment with negative control (0.05% DMSO and 0.05% deionised water), positive control (50 µM quercetin), and various concentrations of MO-AgNPs and ethanol extract of <i>M. oleifera</i> after 10 days. Black arrows indicate blood vessels. Treatment with 12 µg/mL MO-AgNPs significantly inhibited formation of new blood vessels. ....	125
Figure 4.27	The location of angiogenin, IL-8, MCP-1, TIMP-1, TIMP-2, and VEGF angiogenic factors in the human angiogenic antibody array, which were down-regulated. In contrast, Ang-1 and Ang-2 were significantly upregulated in the treated sample. Images were captured using an Agilent G2505C Scanner.....	127
Figure 4.28	Data analysis of the signal intensities of angiogenic factors in the supernatant of EA.hy926 cell line. The data were displayed as a fold change of the treated to untreated samples. The bar graph shows the significant downregulation of angiogenic factors,	

	including angiogenin, IL-8, MCP-1, TIMP-1, TIMP-2, and VEGF ( $\leq 0.65$ -fold and $\geq 1.5$ -fold) after treatment with MO-AgNPs using the human angiogenesis antibody array. ....	127
Figure 4.29	Data analysis of the signal intensities of angiogenic factors in the supernatant of EA.hy926 cell line. The data were displayed as a fold change of the treated to untreated samples. The bar graph shows the significant upregulation of angiogenic factors, including Ang-1 and Ang-2 ( $\leq 0.65$ -fold and $\geq 1.5$ -fold), after treatment with MO-AgNPs using the human angiogenesis antibody array.....	128
Figure 4.30	Binding conformation of 4-p-coumaroylquinic acid-Ag <sub>3</sub> at the binding sites of (a) VEGF, and (b) angiogenin. The figure illustrates the molecular docking results showing how the silver-conjugated ligand (4-p-coumaroylquinic acid-Ag <sub>3</sub> ) interacts within the binding pocket of the target proteins. The ligand is displayed in stick representation (colored by element: carbon in green, oxygen in red, hydrogen in white, and silver in gray). The protein surface and binding pocket are shown in cartoon format for spatial clarity. Color-coded interaction types are visualized as follows: Green dashed lines (Conventional hydrogen bonds), Pale green dashed lines (Van der Waals interactions), Orange dashed lines (Pi-Sigma interactions), Purple dashed lines (Pi-Pi T-shaped interactions), Dark pink dashed lines (Pi-Alkyl interactions). The 3D structure illustrates the protein bound to the bioactive compound, highlighting key interactions that stabilize the complex. ....	130
Figure 4.31	Binding conformation of 2,4-dichlorobenzoate-Ag <sub>3</sub> at the binding sites of (a) VEGF, (b) angiogenin, (c) IL-8, and (d) MCP-1. The figure illustrates the molecular docking results showing how the silver-conjugated ligand (2,4-dichlorobenzoate-Ag <sub>3</sub> ) interacts within the binding pocket of the target proteins. The ligand is displayed in stick representation (colored by element: carbon in green, oxygen in red, hydrogen in white, and silver in gray). The protein surface and binding pocket are shown in cartoon format for spatial clarity. Color-coded interaction types are visualized as follows: Green dashed lines (Conventional hydrogen bonds), Pale green dashed lines (Van der Waals interactions), Orange dashed lines (Pi-Sigma interactions), Purple dashed lines (Pi-Pi T-shaped interactions), Dark pink dashed lines (Pi-Alkyl interactions). The 3D structure illustrates the protein bound to the bioactive compound, highlighting key interactions that stabilize the complex. ....	132
Figure 4.32	Binding conformation of 5-methyl-octanoic acid-Ag <sub>3</sub> at the binding sites of (a) VEGF, (b) IL-8, and (c) MCP-1. The figure illustrates the molecular docking results showing how the silver-conjugated ligand (5-methyl-octanoic acid-Ag <sub>3</sub> ) interacts within the binding pocket of the target proteins. The ligand is displayed	

in stick representation (colored by element: carbon in green, oxygen in red, hydrogen in white, and silver in gray). The protein surface and binding pocket are shown in cartoon format for spatial clarity. Color-coded interaction types are visualized as follows: Green dashed lines (Conventional hydrogen bonds), Pale green dashed lines (Van der Waals interactions), Orange dashed lines (Pi-Sigma interactions), Purple dashed lines (Pi-Pi T-shaped interactions), Dark pink dashed lines (Pi-Alkyl interactions). The 3D structure illustrates the protein bound to the bioactive compound, highlighting key interactions that stabilize the complex. .... 134

Figure 4.33 Binding conformation of R-pantolactone-Ag<sub>3</sub> at the binding sites of (a) VEGF, (b) angiogenin, (c) IL-8, and (d) MCP-1. The figure illustrates the molecular docking results showing how the silver-conjugated ligand (R-pantolactone-Ag<sub>3</sub>) interacts within the binding pocket of the target proteins. The ligand is displayed in stick representation (colored by element: carbon in green, oxygen in red, hydrogen in white, and silver in gray). The protein surface and binding pocket are shown in cartoon format for spatial clarity. Color-coded interaction types are visualized as follows: Green dashed lines (Conventional hydrogen bonds), Pale green dashed lines (Van der Waals interactions), Orange dashed lines (Pi-Sigma interactions), Purple dashed lines (Pi-Pi T-shaped interactions), Dark pink dashed lines (Pi-Alkyl interactions). The 3D structure illustrates the protein bound to the bioactive compound, highlighting key interactions that stabilize the complex. .... 136

Figure 4.34 Free binding energy of the main compounds in MO-AgNPs and positive controls with angiogenic factors (a) 4-p-coumaroylquinic acid, (b) 2,4-dichlorobenzoate-Ag<sub>3</sub>, (c) 5-methyl-octanoic acid- Ag<sub>3</sub>, (d) R-pantolactone-Ag<sub>3</sub>, (e) 3-hydroxydecanoic acid-Ag<sub>3</sub> (conjugate 1), (f) 3-hydroxydecanoic acid-Ag<sub>3</sub> (conjugate 2), (g) Axitinib, (h) Pazopanib, (i) Cabozantinib. .... 139

Figure 4.35 Images of CAM before and after treatment with negative control (0.05% DMSO and 0.05% deionised water), positive control (50 µM quercetin), and 4-p-coumaroylquinic acid at half IC<sub>50</sub>, IC<sub>50</sub>, and double IC<sub>50</sub> for 10 days. Black arrows indicate blood vessels. Treatment with IC<sub>50</sub> 4-p-coumaroylquinic acid effectively inhibited formation of new blood vessels. .... 142

Figure 5.1 Proposed mechanism of anti-angiogenic and anti-inflammatory effects of MO-AgNPs. MO-AgNPs treatment had a significant impact on the expression of angiogenic and inflammatory factors in EA.hy926 cells, downregulating important pro-angiogenic molecules such as VEGF, IL-8, MCP-1, and angiogenin. This disruption inhibits essential signalling pathways required for ECs proliferation, migration, and survival, as well as lowering

inflammatory responses that lead to tumour associated angiogenesis. Note that the display of protein shapes and orientations does not accurately reflect their real structure within cells. This figure was generated using BioRender.com. .... 167

Figure 5.2 Proposed indirect mechanism of anti-angiogenic and anti-inflammatory effects induced by MO-AgNPs in ECs. MO-AgNPs change the microenvironment and signalling pathways of ECs, indirectly modulating angiogenic and inflammatory processes. The MO-AgNPs reduces the expression of critical pro-angiogenic factors such as VEGF, IL-8, MCP-1, and angiogenin, altering the signals that ECs use for proliferation, migration, and tube formation. The decrease in pro-angiogenic factors impairs the endothelial response to angiogenic stimuli, reducing the development of new blood vessels and reducing the inflammatory responses that drive tumour associated angiogenesis, whereas the Ang-1 balance promotes vascular stability and prevents aberrant angiogenesis. Note that the representation of protein shapes and orientations does not accurately reflect their real structure within cells. This figure was generated with BioRender.com. .... 168

## LIST OF SYMBOLS

$\alpha$	Alpha
$\beta$	Beta
$\delta$	Delta
$\kappa$	Kappa
$^{\circ}\text{C}$	Degree Celsius
%	Percent

## LIST OF UNITS

cm	Centimetre
g	Gram
hr	Hour
kg	Kilogram
L	Liter
m	Meter
M	Molar
mg	Milligram
min	Minute
mL	Milliliter
mm	Millimeter
mm <sup>3</sup>	Cubic millimetre
mM	Millimolar
mmol	Millimole
nm	Nanometre
rpm	Revolution per minute
µg	Microgram
µL	Microliter

## LIST OF ABBREVIATIONS

Ang	Angiopoietin
Å	Angstrom
AgNO <sub>3</sub>	Silver Nitrate
AgNPs	Silver Nanoparticles
Akt	Protein Kinase B
ASR	Age-Standardized Incidence Rates
ATCC	American Type Culture Collection
AuNPs	Gold Nanoparticles
Bcl-2	B-cell Lymphoma 2
Ca	Calcium
CAM	Chorioallantoic Membrane
CCR2	C-C Chemokine Receptor Type 2
CIMP	CpG Island Methylator Phenotype
CIN	Chromosomal Instability
CLSM	Confocal Laser Scanning Microscopy
COX-2	Cyclooxygenase-2
CRC	Colorectal Cancer
CXC	Chemokine
CXCR	Chemokine Receptor
DDS	Drug Delivery System
DLS	Dynamic Light Scattering
DMEM	Dulbecco 's Modified Eagle Medium
DNA	Deoxyribonucleic Acid

ECs	Endothelial Cells
ECM	Extracellular Matrix
EGF	Epidermal Growth Factor
EGFR	Epidermal Growth Factor Receptor
ERK	Extracellular Signal-Regulated Kinase
FBS	Fetal0 Bovine Serum
FGF	Fibroblast Growth Factor
5-FU	Fluorouracil
Grb2	Growth Factor Receptor-bound Protein 2
HIF-1 $\alpha$	Hypoxia Inducible Factor
HPLC	High-Performance Liquid Chromatography
HT29	Human colorectal adenocarcinoma cell line
IL	Interleukin
IACUC	Institutional Animal Care and Use Committee
MAPK	Mitogen-activated protein kinase
mCRC	Metastatic Colorectal Cancer
MEK	Mitogen-Activated Protein Kinase/ERK Kinase
MMPs	Matrix Metalloproteinases
MMPIs	Matrix Metalloproteinase Inhibitors
MO	<i>Moringa oleifera</i>
MO-AgNPs	<i>Moringa oleifera</i> -Silver Nanoparticles
MS/MS	Double Mass spectrometry
MSI	Microsatellite Instability
MTT	3-(4,5-Dimethylthiazol-2-yl)-2,5-Diphenyl Tetrazolium Bromide
NCI	National Cancer Institute

NO	Nitric Oxide
NPs	Nanoparticles
NSCLC	Non-Small Cell Lung Cancer
PBS	Phosphate Buffer Solution
PDB	Protein Data Bank
PDGF	Platelet-Derived Growth Factor
PDI	polydispersity Index
PIGF	Placental Growth Factor
PI3K	Phosphoinositide 3-Kinase
PKC	Protein Kinase C
PLC	Phospholipase C
PMT	Photomultiplier Tube
QTOF	Quadrupole Time of Flight
Raf	Rapidly Accelerated Fibrosarcoma
Ras	Rat Sarcoma
RCSB	Research Collaboratory for structural Bioinformatics
SDI	Socio-Demographic Index
RNase	Ribonuclease 5
ROS	Reactive Oxygen Species
SEM	Scanning Electron Microscopy
TEM	Transmission Electron Microscopy
TGF	Transforming Growth Factor
Tie-2	Receptor Tyrosine Kinase
3D	Three Dimensional
TKIs	Tyrosine Kinase Inhibitors

TME	Tumour Microenvironment
2D	Two Dimensional
UV- Vis	UV- Visible
VEGF	Vascular Endothelial Growth Factor
VEGFR	Vascular Endothelial Growth Factor Receptor
WHO	World Health Organization

## LIST OF APPENDICES

- Appendix A      Ethical approval  
                    Certificate gold award  
                    Certificate silver award
- Appendix B      HPLC-MS/MS Chemical Identification Report of before and after  
                    synthesis of MO-AgNPs
- Appendix C      Comprehensive Analysis of Molecular Docking Simulations

**POTENSI FARMAKOLOGI NANOPARTIKEL PERAK  
*MORINGA OLEIFERA* MENYASAR ANGIOGENESIS DAN  
RENCATAN TITISAN SEL KANSER KOLOREKTAL**

**ABSTRAK**

Ejen anti-angiogenik daripada sumber semula jadi adalah calon yang menjanjikan untuk terapi kanser. Memandangkan kurangnya penyelidikan tentang sifat terapeutik luar biasa ekstrak *M. oleifera*, kajian ini bertujuan untuk menilai potensi farmakologi nanopartikel perak *M. oleifera* (MO-AgNPs) dalam menghalang dan mengganggu proses neovaskularisasi dalam saluran sedia ada (angiogenesis) dalam sel kanser kolorektal. Sintesis nanopartikel bermula dengan pengestrakan berurutan daripada daun *M. oleifera*, diikuti dengan penambahan larutan perak nitrat 1mM (AgNO<sub>3</sub>) untuk membentuk MO-AgNPs dengan saiz zarah purata  $57.88 \pm 4.06$  nm, dan potensi zeta -15.9 mV. Spektroskopi UV-Vis telah digunakan untuk mengesahkan kewujudan MO-AgNPs, yang ditunjukkan melalui kehadiran satu puncak serapan yang jelas pada panjang gelombang 430 nm. Identiti kimia ekstrak akueus *M. oleifera* dengan skor tertinggi dan kualiti data yang memadai dikenal pasti menggunakan analisis HP-LC-MS/MS QTOF. Antara kompaun yang dikenal pasti termasuklah asid 2,4-diklorobenzoat, Merodesmosine, ptelatoside A, R- pantolakton, asid 5-methyl-octanoic dan 4-p-Coumaroylquinic. MO-AgNPs menunjukkan IC<sub>50</sub> berganda dalam sel selanjara endothelial berbanding sel selanjara kanser kolorektal dalam ujian MTT, dengan IC<sub>50</sub> masing-masing pada 12 dan 5.5 µg/mL. Perubahan morfologi dalam sel menunjukkan kesan antiangiogenik MO-AgNPs yang bergantung kepada dos. Selain itu, kepekatan optimum MO-AgNPs pada 12 µg/mL menyebabkan kematian sel dalam ujian kolonogenik, dengan peratus perencatan pembentukan koloni sebanyak 51.5%

( $p \leq 0.01$ ) dan peratus perencatan penutupan yang ketara sebanyak 63.1% ( $p \leq 0.01$ ). Pengurangan pencerobohan sel dan penghalangan pembentukan tiub endothelial masing-masing mencapai 62.1% (p-nilai  $\leq 0.01$ ) dan 100%, menunjukkan kesan yang bergantung kepada dos. Berdasarkan keputusan kajian ini, kesan antiangiogenik diperhatikan pada dos 12  $\mu\text{g/mL}$  MO-AgNPs dengan peratusan perencatan tertinggi terhadap pembentukan neovaskularisasi, iaitu  $83.824 \pm 0.081$  (p-nilai  $\leq 0.01$ ) dalam ujian aorta tikus. Selepas 14 hari rawatan, aktiviti anti-tumour MO-AgNPs terhadap model sferoid 3D dalam kultur in vitro menunjukkan bahawa dos 12  $\mu\text{g/mL}$  boleh mengehadkan perkembangan sferoid sebanyak  $83 \pm 0.158\%$  (p-nilai  $\leq 0.05$ ) berbanding kumpulan yang tidak dirawat. Ujian membran korioallantoik (CAM) turut menunjukkan kesan antiangiogenik tambahan, dengan penindasan proses pembangunan vaskularisasi yang ketara pada dos 12  $\mu\text{g/mL}$  MO-AgNPs. Analisis molekul menunjukkan pengurangan faktor angiogenik utama, seperti VEGF, IL-8, Angiogenin, dan MCP-1, manakala Angiopoietin dikawal selia. Kajian 'docking' menunjukkan potensi interaksi MO-AgNPs dengan reseptor yang terlibat dalam angiogenesis. Ujian MTT dan CAM mengesahkan sifat anti-angiogenic asid 4-p-Coumaroylquinic yang menunjukkan afiniti pengikatan tertinggi ( $-8.48$  kcal/mol) terhadap VEGF dalam kajian 'docking'. Kesimpulannya, MO-AgNPs berpotensi sebagai agen antiangiogenik, yang dapat mengganggu proses berkaitan angiogenesis, melalui perencatan faktor angiogenik seperti VEGF, IL8, Angiogenin, dan MCP-1 oleh sebatian bioaktif asid 4-p-Coumaroylquinic, 2,4-diklorobenzoat, R-pantolactone dan asid 5-methyl-octanoic. Penemuan ini berpotensi menyumbang kepada pembangunan terapeutik yang disasarkan bagi gangguan angiogenik dan penyakit berkaitan.

**PHARMACOLOGICAL POTENTIAL OF *MORINGA OLEIFERA*  
SILVER NANOPARTICLES TARGETING ANGIOGENESIS AND  
COLORECTAL CANCER CELL LINES INHIBITION**

**ABSTRACT**

Anti-angiogenic agents from natural sources are promising candidates for cancer therapy, especially when formulated through nanotechnology approaches, which are considered a modern and promising field for treating various hard to control cancers. This study aims to evaluate the potential of *M. oleifera* silver nanoparticles (MO-AgNPs) in inhibiting and disrupting neovascularisation in existing vessels (angiogenesis). The MO-AgNPs were first synthesised through a sequential extraction of *M. oleifera* leaves, followed by the addition of 1 mM silver nitrate (AgNO<sub>3</sub>) solution. The characterisation analysis showed that the nanoparticles had an average particle size of  $57.88 \pm 4.06$  nm and a zeta potential of -15.9 mV, with distinct peaks observed at 430 nm through UV-Vis spectrophotometry, confirming the presence of MO-AgNPs. Subsequently, the chemical composition of *M. oleifera* aqueous extract was assessed using HPLC-MS/MS QTOF analysis, which identified the presence of 4-p-coumaroylquinic acid, 2,4-dichlorobenzoate, merodesmosine, pteleoside A, R-pantolactone, and 5-methyl-octanoic acid. Based on the MTT assay, the half-maximal inhibition concentration (IC<sub>50</sub>) of MO-AgNPs in endothelial cells was twice higher (12 µg/mL) compared to in colorectal cancer cells (5.5 µg/mL). MO-AgNPs also exhibited concentration-dependent anti-angiogenic effects and induced morphological changes in cells. Furthermore, the optimal concentration of MO-AgNPs at 12 µg/mL caused cell death in the clonogenic assay, with a significant inhibition of colony formation (51.5%,  $p \leq 0.01$ ) and a significant closure inhibition percentage of 63.1% ( $p \leq 0.01$ ). Treatment

with MO-AgNPs also achieved a reduction of cell invasion and inhibition of endothelial tube formation of 62.1% (p-value  $\leq 0.01$ ) and 100%, respectively, following a dose-dependent pattern. Moreover, MO-AgNPs at 12  $\mu\text{g/mL}$  concentration recorded the highest percentage of inhibition in neovascularisation formation of  $83.824 \pm 0.081$  (p-value  $\leq 0.01$ ) in the rat aortic assay after 14 days of treatment. Additionally, the anti-tumour activities of MO-AgNPs at 12  $\mu\text{g/mL}$  against in vitro co-cultured 3D spheroids model impeded the spheroids' development by  $83 \pm 0.158\%$  (p-value  $\leq 0.05$ ) compared to the untreated group. Besides, the Chorioallantoic Membrane (CAM) experiment demonstrated notable suppression of the vascularisation development using 12  $\mu\text{g/mL}$  of MO-AgNPs. Molecular analysis revealed the downregulation of vital angiogenic factors, such as Vascular Endothelial Growth Factor (VEGF), interleukin-8 (IL-8), angiogenin, and Monocyte Chemoattractant Protein-1 (MCP-1), in contrast to the upregulation of angiopoietins. Further docking studies indicated the potential interactions of MO-AgNPs' major compounds with receptors involved in angiogenesis. Remarkably, the MTT and CAM assays confirmed the anti-angiogenic properties of 4-p-coumaroylquinic acid, which recorded the highest binding affinity of -8.48 kcal/mol towards VEGF in the docking assay. In conclusion, MO-AgNPs showed promising application as an exceptional anti-angiogenic agent that can disrupt angiogenesis-related processes through the inhibition of angiogenic factors, such as VEGF, IL-8, angiogenin, and MCP-1, through its bioactive compounds, including 4-p-coumaroylquinic acid, 2,4-dichlorobenzoate, R-pantolactone, and 5-methyl-octanoic acid. This can potentially contribute to developing targeted therapeutics for angiogenic disorders and related diseases.

# CHAPTER 1

## INTRODUCTION

### 1.1 Research Background

Cancer diseases remain the primary cause of death worldwide and involve the highest treatment costs, impacting individuals and governmental entities across all genders, ages, races, and ethnicities (Workie *et al.*, 2023). Despite the revolutionary developments in both diagnosis and treatment of cancer disease, it is projected that the medical cost for curing cancers will rise by 34%, up to \$246 billion in 2030 compared to \$183 billion in 2015 in the United States of America (USA) (Mariotto *et al.*, 2020).

According to the World Health Organisation (WHO) statistics in 2022, Malaysia recorded 48,639 new cancer cases in 2020 alone, and the number is expected to double by 2040. As such, 1 in 10 Malaysians will be diagnosed with cancer during their lifetime (Ganeson *et al.*, 2023). Adult-onset colorectal cancer (CRC) (diagnosed at age  $\geq 50$  years) accounted for 79.6% of all cases of CRC, significantly more prevalent than young-onset CRC (diagnosed before age 50) at 20.4%. CRC was more common in men at 53.9% and the Malay sub-population at 90.2% of all cases. As a developing country in Southeast Asia, Malaysia has experienced a rising trend in CRC incidence over the years. The Malaysian National Cancer Registry reported an increase in CRC incidence from 13.2% between 2007-2011 to 13.5% between 2012-2016. Additionally, the International Agency for Research on Cancer projected that Malaysia would have 6,597 new CRC cases 13.6% and 3,420 CRC-related deaths 11.6% by 2020 (Isah Tsamiya *et al.*, 2024). The Malaysian National Cancer Registry determined that the most prevalent tumours documented in Malaysia are leukemia, colon cancer, lung cancer, breast cancer, and ovarian cancer (Mustafa *et al.*, 2022).

CRC is the most prevalent cancer in men 16.9% of all diagnosed cancers, and the second most common in women 10.7% of the total cancer cases in Malaysia (Nawawi *et al.*, 2021). The disease represents a substantial economic burden, which is projected to increase steadily in the future due to the prevailing trends in its occurrence. The majority of individuals diagnosed with CRC are identified at an advanced stage, resulting in a survival rate of 5 years that is less favourable compared to other developed Asian nations. This lower rate of survival may be linked to poor public awareness of CRC and low participation rates in cancer screening programs (Muhamad *et al.*, 2023).

The exorbitant cost of treating this disease necessitates researchers to explore further and develop different therapeutics strategies, such as anti-angiogenesis agents, which have proven to exhibit promising properties against several types of solid cancers (Lopes-Coelho *et al.*, 2021). Moreover, exploring the secrets of natural compounds, which are rich in therapeutic properties, and developing new drug delivery techniques, such as silver nanoparticles (AgNPs), could also lead to adequate, safe, and biocompatible treatment (K Karunakar *et al.*, 2024).

## **1.2 Angiogenesis**

Angiogenesis refers to the development of new capillaries through cellular outgrowth from pre-existing micro-vessels. The multi-step angiogenesis process involves a wide range of angiogenic factors and inhibitors, providing numerous targets for therapeutic interventions and imaging (Hosseini, Shafieian and Alipour, 2022). However, defective angiogenesis has been linked to the development of several diseases, such as vascular retinopathies, rheumatoid arthritis, and cancer. The idea that tumour development relies on neo-angiogenesis has been convincingly established through the pioneering work of Folkman and his colleagues (Folkman, 2023).

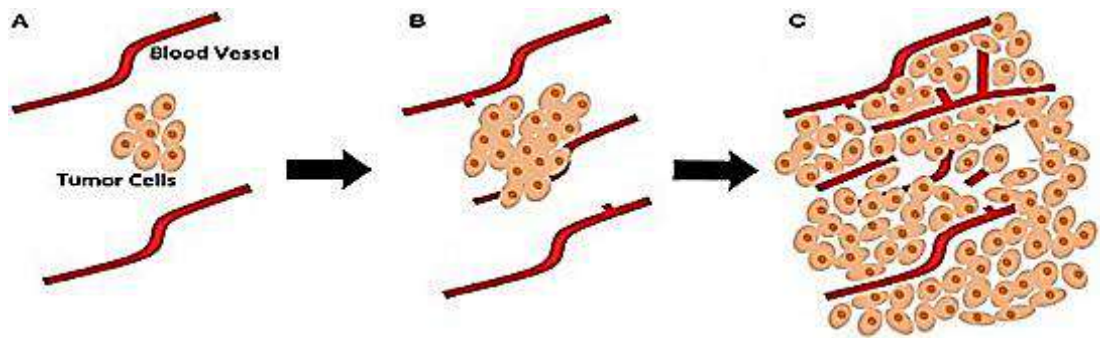


Figure 1.1 The role of sprouting angiogenesis in tumour development. (A) During the early stages of growth, the tumour is very small and depends on existing blood arteries for oxygen and nutrients. (B) As the tumour expands, new vessels sprout from local existing blood vessels to meet the increased demand for oxygen and nutrients. (C) Sprouting angiogenesis creates a more complicated structure of vascular to ensure enough blood supply to the expanding tumour (Haibe *et al.*, 2020).

The identification of members of growth factor families in past research marks a significant advancement in identifying angiogenic chemicals (Folkman, 2023). These growth factors include epidermal growth factor (EGF), transforming growth factor (TGF), platelet-derived growth factor (PDGF), VEGF, and fibroblast growth factor (FGF). Such discoveries have advanced the current knowledge of angiogenesis, a process regulated by multiple regulatory and signalling molecules (Ting *et al.*, 2021).

Solid tumours can grow up to 2 mm<sup>3</sup> without vascularization; however, they rely on blood vessels to provide sufficient oxygen and nutrients for further growth (Bungărdean *et al.*, 2023). Various mechanisms contribute to neovascularisation in tumours, including angiogenesis, vessel co-option, vascular mimicry, trans-differentiation of cancer cells into endothelial cells (ECs), and recruitment of endothelial progenitor cells (Hooglugt *et al.*, 2021).

Angiogenesis involves several distinct stages. Initially, pro-angiogenic factors are released into the surrounding extracellular fluid, which activates ECs. Subsequently, these ECs migrate towards areas of high pro-angiogenic factor concentration, where they adhere or bind to existing vasculature and contribute to the formation of a fully

functional network of blood vessels (Laschke, Gu and Menger, 2022). Tumour tissues have a higher tendency to promote angiogenesis, with blood vessels primarily composed of ECs. Blood capillaries in normal tissues may expand when blood flow or oxygen levels are reduced, leading to elevated capillary permeability and fibrin exudation. Concurrently, collagenase activation and basement membrane disruption contribute to the restructuring of the extracellular matrix (ECM). Moreover, angiogenic factors stimulate the growth and division of ECs, which form tubular structures that create new blood vessels within the tumour (Jiang *et al.*, 2020).

This mechanism of action encourages researchers to develop new targeting medications using targeted drug delivery systems (DDS), such as nanomaterials, to suppress or enhance this mechanism according to required therapeutic concerns.

### **1.3 Silver Nanoparticles**

Since the late 1960s and early 1970s, the theoretical concept of nanomaterials has expanded tremendously and is practically employed in various fields, including disease treatment and prevention of health-related problems across multiple indications and properties (Abid *et al.*, 2022). Compared to existing approaches, nanomaterials offer several advantages in the medical field, including minimal drug exposure, diminished side effects, enhanced bioavailability, lower financial burden of therapy, and improved patient compliance to treatment (Takáč *et al.*, 2023).

Nanoparticles possess a substantially large surface area-to-volume ratio that contributes to their improved physical and chemical characteristics. They are utilised in diverse domains, including antimicrobial research, new anti-angiogenic herbal medications, bio-molecular detection, diagnostic applications, catalytic processes,

advanced microelectronics, highly sensitive sensing devices, and DDS targeting tumour cells (Raju and Ying, 2023; Ahmad *et al.*, 2024).

Plants have been utilised in the synthesis of metal nanoparticles, including silver, due to their unique characteristics and practical uses. Silver is a particularly significant element owing to its distinctive characteristics, such as excellent physical properties, abundantly available at low cost, ease of use, high conductivity, chemically stable, and robust catalytic and antibacterial activity. Despite being less than 50 nm in size, these metal nanoparticles can deliver large therapeutic dosages due to their large surface area (Aouf *et al.*, 2024).

#### **1.4 *Moringa oleifera***

*M. oleifera*, also referred to as drumstick tree, ben oil tree, horseradish tree, wonder tree, or simply *Moringa*, belongs to the *Moringaceae* family (Jattan *et al.*, 2021; Pareek *et al.*, 2023). This shedding-leaves plant is native to south Asia and has many medical uses. Traditionally, *M. oleifera* is used as a stimulant, anti-spasmodic, diuretic, expectorant, abortifacient, antifungal, antiviral, anti-inflammatory, and antibacterial. It is also applied to increase the flow of bile and cardiac circulatory tonic. Besides, it possesses antiseptic, antipyretic, and anti-diabetic properties (Adji *et al.*, 2022; Oyeyinka *et al.*, 2022).

*M. oleifera* can also be used as an anti-epileptic to cure nervous debility, asthma, and enlarged liver and spleen, as a gargle to treat hoarseness and sore throat, as an anti-paralytic to alleviate hiccups (emetic in high doses) and provide relief in influenza (Ercan, 2022). Interestingly, the Ayurvedic pharmacopoeia of India has also described the use of the almost *M. oleifera* parts: root, bark, gum, leaf, fruit (pods), flowers, seeds,

and seed oil to treat goitre, heart problems, rheumatism bronchitis, and wounds (Milla, Peñalver and Nieto, 2021).

Recent studies have revealed that *M. oleifera* exhibits several potent therapeutic properties, such as antimicrobial, anti-inflammatory, antioxidant, antipyretic and wound-healing, anti-cancer, and analgesic effects (Ramamurthy *et al.*, 2022; Klimek-Szczykutowicz *et al.*, 2024). *M. oleifera* has also demonstrated anti-angiogenic properties that warrant further research and development to realise the use of *M. oleifera* as a promising and modern therapeutic agent (Thongrungs *et al.*, 2022).

## 1.5 Problem Statement

Angiogenesis is critical for tumour growth and expansion as it involves the formation of new blood vessel networks to supply adequate oxygen and nutritional requirements to the new cells. Key angiogenic factors derived from the ECs, such as VEGF, are released to stimulate the process (Torshizi Esfahani *et al.*, 2024). In view of this, recent studies have reported that anti-angiogenic medications, such as quercetin and suramin, can significantly inhibit tumour growth but may lead to enhanced tumour cell adaptation and resistance due to the upregulation of alternative angiogenic factors. Besides, these medications exhibit poor bioavailability in the targeted tissues (Sadalage *et al.*, 2021; Zhao *et al.*, 2024).

Although *M. oleifera* is widely known for its expansive medicinal properties and applications (Zarina *et al.*, 2024), a clear research gap exists regarding its unexplored antiangiogenic potential, particularly in solid tumours such as CRC, which remains one of the leading causes of cancer-related deaths worldwide (Hibino *et al.*, 2021). Meanwhile, the exceptional features of AgNPs have been exploited in many

therapeutic researches, such as cancer treatment through the inhibition of angiogenesis, which is a relatively new area of research (Karunakar *et al.*, 2024). However, the specific mechanisms by which AgNPs, especially those synthesized using *M. oleifera*, affect angiogenesis and inhibit tumour progression remain largely unclear. Furthermore, limited studies have identified or characterized the bioactive compounds within *M. oleifera* silver nanoparticles (MO-AgNPs) that may interact with key angiogenic regulators such as VEGF, IL-8 and MCP-1.

New anti-angiogenic agents are being developed based on the various molecular structures of natural phytochemicals (Lim, Chan and Hamid, 2024). Botanical extracts contain a complex array of organic compounds that can target multiple angiogenic pathways to reduce drug resistance through compensatory mechanisms. Therefore, this study addresses the existing research gap by investigating the antiangiogenic activity of MO-AgNPs and their specific bioactive components, focusing on their molecular interactions with key angiogenic proteins and signaling pathways. This research aims to contribute to the development of novel antiangiogenic therapeutics by elucidating how MO-AgNPs can suppress endothelial cell driven angiogenesis and inhibit CRC progression through multi-targeted molecular mechanisms.

## **1.6 Objective of the Study**

### **1.6.1 Main Objective**

This study objective to assess the anti-angiogenesis properties of MO-AgNPs for potential treatment against CRC cell lines.

### 1.6.2 Specific Objective

In order to fulfil the main objective of this study, the following specific objectives were established:

1. To synthesise MO-AgNPs from *M. oleifera* and characterise their physicochemical properties.
2. To evaluate the anti-angiogenic effect of MO-AgNPs against endothelial cell lines through in vitro, ex vivo, and mimic in vivo processes.
3. To identify the molecular effect and active compound(s) in MO-AgNPs responsible for the anti-angiogenic response.
4. To perform molecular docking analysis to predict the binding conformations of key angiogenic factors with the active compound(s) in MO-AgNPs and verify their potential anti-angiogenic effects.

### 1.7 Research Questions

Several research questions were developed to define the scope and direction of this study, as well as to formulate the proposition of this study. These questions include:

1. Can MO-AgNPs be synthesised from *M. oleifera* and what are their physicochemical properties?
2. Does MO-AgNPs exhibit significant anti-angiogenic properties?
3. What are the molecular effects and active compound(s) responsible for the anti-angiogenic response of MO-AgNPs?

4. What is the binding affinity of the bioactive compounds in MO-AgNPs toward their target sites, and do molecular docking results practically confirm their anti-angiogenic effects?

## **1.8 Research Hypothesis**

Null Hypothesis ( $H_0$ ):

MO-AgNPs do not significantly inhibit angiogenesis in CRC cell lines, and no specific active compounds in MO-AgNPs are responsible for an anti-angiogenic effect. Additionally, the molecular docking of bioactive compounds in MO-AgNPs does not predict strong or relevant binding interactions with angiogenesis-related target proteins, and any observed docking effects do not translate to practical anti-angiogenic outcomes.

Alternative Hypothesis ( $H_1$ ):

MO-AgNPs significantly inhibit angiogenesis in CRC cell lines, and specific active compounds in MO-AgNPs are responsible for this anti-angiogenic effect. Molecular docking of these bioactive compounds predicts strong and relevant binding interactions with angiogenesis-related target proteins, which are further confirmed by practical anti-angiogenic effects in in vitro, ex vivo, and mimic in vivo models.

## **CHAPTER 2**

### **LITERATURE REVIEW**

#### **2.1 Introduction to Cancer and Its Therapy**

Cancer is a collective term for diseases marked by the uncontrolled proliferation and spread of abnormal cells. These cells can invade nearby tissues and metastasize to other areas of the body via the bloodstream and lymphatic system, potentially leading to death. Cancer can emerge in nearly any part of the body and is categorized based on the type of cell or organ in which it originates. Various factors contribute to the development of cancer, including genetic mutations, environmental exposures, and lifestyle factors. Early detection of tumours and effective treatment are crucial for improving survival rates and the quality of life for those affected (Yadav and Mohite, 2020).

The hallmarks of cancer provide an explanation for understanding how the disease progresses. Maintaining proliferative signals, avoiding growth suppressors, preventing cell death, permitting immortality through replication, triggering angiogenesis, and initiating invasion and metastasis are some of these characteristics. Because of these characteristics, cancer cells can proliferate and outcompete healthy cells, which results in the development of tumours and their spread (Hanahan, 2022).

A critical factor in cancer progression is angiogenesis, the process of forming new blood vessels. Tumours depend on this vascular network to supply oxygen and essential nutrients. Without this vascular network, tumours would be limited in size. Angiogenesis not only facilitates tumour growth but also permits cancer cells to invade adjacent tissues and enter the bloodstream, initiating metastasis. The capability of

cancer cells to metastasize to distant organs remains a main challenge in cancer therapy and a leading cause of cancer-related mortality (Folkman, 2023).

### **2.1.1 Mechanisms of Tumour Growth and Metastasis**

The development of tumours starts when cellular abnormalities cause uncontrolled proliferation of cells by interfering with the regulatory processes that regulate cell division. These cells gradually get new mutations that strengthen their capacity to invade neighboring organs. A number of processes are involved in metastasis, including local invasion, intravasation into lymphatic or blood arteries, circulation survival, extravasation into distant tissues, and colonization at secondary sites. Angiogenesis is essential for allowing tumours to grow larger than they need to and for creating a pathway for their metastatic distribution. Tumour development and metastasis are further facilitated by interactions with the ECM and immune evasion mechanisms (Majidpoor and Mortezaee, 2021; Weiss, Lauffenburger and Friedl, 2022).

### **2.1.2 Conventional Approaches to Cancer Treatment**

Standard cancer treatments, including surgery, radiation, and chemotherapy, are still widely used for many cancers. Surgery aims to physically remove tumours, while chemotherapy uses cytotoxic agents to kill rapidly dividing cells. However, both approaches have limitations. Surgery may not be effective for metastatic cancer, and chemotherapy often results in severe side effects due to its lack of specificity, damaging healthy cells in addition to cancer cells (García-Fernández, Fornaguera and Borrós, 2020).

A more recent strategy is targeted therapies, which use medications made to block particular molecular targets used in the development of cancer, such as oncogenic

proteins or growth factor receptors. However, recurrence of the condition is commonly caused by treatment resistance. Furthermore, many cancer types are harder to treat with this method because they lack well-defined targets (Zhong *et al.*, 2021).

### **2.1.3 Innovative Cancer Therapies**

The investigation of natural products and innovative technologies, such as nanomedicine, has been encouraged by the weaknesses of existing treatments. Plant-based alkaloids, polyphenols, and flavonoids are examples of natural substances that have demonstrated promise in preventing angiogenesis, metastasis, and tumour formation. These substances can target several pathways at once and frequently show less toxicity than synthesized medications (Kumar and Sharma, 2023).

One promising method for treating cancer is nanomedicine, which uses nanoparticles to deliver medications or therapeutic substances. Anti-cancer drugs' bioavailability and targeted distribution can be improved using nanoparticles, which also lessens side effects and increases effectiveness. AgNPs have demonstrated anti-cancer effects by inducing apoptosis, inhibiting cell division, and disrupting angiogenesis. Combining natural products with nanotechnology offers significant potential to enhance cancer treatment outcomes by targeting tumour cells more precisely while minimizing damage to healthy tissues (Jabeen *et al.*, 2021).

## **2.2 Colorectal Cancer**

CRC is a significant global public health issue. In 2020, the WHO reported that CRC is the third most prevalent cancer, accounting for around 1.9 million new cases (10% of all cancers) and the second leading cause of cancer-related deaths, with approximately 900,000 fatalities (9.4% of all cancer deaths) worldwide. Approximately

70% of CRC cases are found in countries with a very high Human Development Index, where 1.7 million new cases and 800,000 deaths were reported. Asia recorded the highest number of CRC cases, with nearly 1 million new diagnoses and 500,000 deaths (Medvedeva *et al.*, 2022; Ilic and Ilic, 2024).

In 2019, the highest age-standardized incidence rates (ASR) of CRC were observed in countries with high Socio-Demographic Index (SDI), at 42.8 per 100,000 people, while the lowest rates were seen in low SDI countries, at 7.7 per 100,000. High ASRs were particularly noted in regions such as Australasia, high-income Asia Pacific, and North America, while sub-Saharan Africa and South Asia had the lowest ASRs. From 1990 to 2019, global CRC incidence ASRs significantly increased in both sexes. Among people aged 15-49, the rate rose by 1.7% annually, from 3.5 to 5.7 per 100,000. For those aged 50-69, the increase was 0.7% per year, and for those aged 70 and above, it was 0.5% per year. Middle SDI countries saw the steepest rise, with rates increasing by 2.8% annually, from 10.2 to 20.9 per 100,000. However, incidence rates declined in High-income North America (-0.6% per year) and Australasia (-0.5% per year). The East Asia region experienced the highest increase, with a 3.6% annual rise from 12.8 to 30.9 per 100,000, followed by the Andean Latin America region, which saw a 2.7% annual increase from 10.0 to 20.0 per 100,000 (Ilic and Ilic, 2024).

As a developing nation in Southeast Asia, Malaysia has experienced a rising trend in CRC over the years. The Malaysian National Cancer Registry reported an increase in CRC incidence from 13.2% between 2007 and 2011 to 13.5% from 2012 to 2016. Furthermore, the International Agency for Research on Cancer projected that in 2020, Malaysia would have 6,597 new CRC cases 13.6% and 3,420 deaths 11.6% across all sexes and age groups (Isah Tsamiya *et al.*, 2024).

The risk of CRC is increased by a number of variables. Certain genetic mutations, inflammatory bowel illness, age, and a family history of CRC are known risk factors. The development of CRC is also greatly influenced by lifestyle choices, including smoking, excessive alcohol use, a high-fat, low-fiber diet, and a lack of physical activity (Aleksandrova *et al.*, 2021).

### **2.2.1 Pathogenic Mechanisms in Colon Cancer Development**

CRC is a heterogeneous disease characterized by three primary molecular mechanisms; chromosomal instability (CIN), microsatellite instability (MSI), and the CpG island methylator phenotype (CIMP). Chromosomal instability (CIN), the most common feature, is present in approximately 85% of all CRCs. This pathway involves mutations in key genes that regulate cell growth, found in about 15% of CRC cases, results from defects in DNA mismatch repair mechanisms, leading to genetic mutations. The CIMP pathway is associated with widespread gene silencing due to abnormal DNA methylation (Alzahrani, Al Doghaither and Al-Ghafar, 2021).

### **2.2.2 Treatment Modalities for Colorectal Cancer**

Surgery serves as the cornerstone for treating localized CRC, especially when the disease is detected at an early stage and has not yet metastasized. Surgical resection of the tumour can lead to a high cure rate, making it a preferred option in such cases (Riis, 2020). In many situations, chemotherapy is employed alongside surgery, particularly when cancer has spread beyond the initial site or when there is a significant risk of recurrence. While chemotherapy can be effective, it does come with notable limitations, including toxic side effects and the potential for the cancer to develop resistance to treatment. As a result, patients undergoing chemotherapy must be closely

monitored to manage adverse effects and optimize overall treatment outcomes (Chen, Zheng and Wu, 2021).

Another important treatment option is radiation therapy, which utilizes high-energy particles or waves to target and eliminate cancer cells. This modality is commonly applied in cases of rectal cancer and can be used either before or after surgical procedures. Preoperative radiation therapy aims to reduce tumour size, while postoperative radiation helps prevent recurrence. It is broadly used alone or combined with other therapies (Gavas, Quazi and Karpiński, 2021).

In recent years, targeted therapies have emerged as a significant advancement in cancer treatment. These therapies are designed to specifically interfere with molecular targets involved in tumour growth and survival. Through focusing on particular pathways, targeted therapies often produce fewer side effects compared to traditional chemotherapy. For CRC, agents that target the VEGF and the epidermal growth factor receptor (EGFR) are frequently utilized (Alzahrani, Al Doghaither and Al-Ghafar, 2021). Additionally, anti-angiogenic therapy plays a crucial role in cancer treatment by inhibiting the formation of new blood vessels that tumours require for growth and metastasis. Medications like bevacizumab, sunitinib, and aflibercept target the VEGF pathway, effectively slowing tumour progression by limiting the blood supply to cancerous cells (Haibe *et al.*, 2020).

Furthermore, innovative approaches such as hyperthermia and laser therapy are being explored as adjunct treatments. Hyperthermia involves heating cancer tissues to destroy malignant cells while sparing healthy ones, and although it is still under investigation, this method shows promise, especially when combined with other treatments (Szwed and Marczak, 2024). On the other hand, laser therapy employs

precise laser beams to remove or shrink tumours, proving particularly useful in cases where conventional surgical methods may pose challenges (Fan *et al.*, 2024).

### **2.2.3 Novel Therapeutic Approaches for Colorectal Cancer**

Nanotechnology has attracted a lot of interest in the treatment of cancer because it can improve drug delivery, increase efficacy, and reduce adverse effects. Chemotherapy medications can be delivered precisely to tumour cells via nanoparticles, protecting healthy tissues in the process. AgNPs in particular have shown promise in causing CRC cells to undergo apoptosis, preventing angiogenesis, and overcoming treatment resistance. Controlled drug release is another benefit of this strategy, which enhances therapy results overall (Guo *et al.*, 2022).

Natural products are increasingly being integrated into cancer therapy alongside traditional treatments due to their potential to enhance treatment efficacy and reduce toxicity. *M. oleifera* and other phytopharmaceuticals have shown promise in the treatment of CRC because of their bioactive constituents, which include phenolic acids and flavonoids. These compounds influence crucial biological mechanisms implicated in cancer, such as angiogenesis, cell cycle regulation, and apoptosis. For instance, *M. oleifera* exhibits anti-cancer properties through its anti-inflammatory, anti-angiogenic, and antioxidant activities, making it a valuable supplement to conventional treatments (Aboulthana *et al.*, 2021).

### **2.3 Angiogenesis: A Crucial Process in Cancer Progression**

Angiogenesis, the formation of new blood vessels, is a critical process in both physiological and pathological conditions. During wound healing, mechanical stimuli from distorted blood vessels and ECM interactions trigger EC multiplication and

capillary budding. This is facilitated by tissue stretching, leading to ischemia, which activates the hypoxia-inducible factor (HIF-1 $\alpha$ ) pathway. In response, VEGF is released, stimulating EC proliferation and promoting new vessel formation (Sharma *et al.*, 2021). Angiogenesis also plays a vital role in embryonic development, where VEGFR2 and VEGFR1 are required sequentially for blood vessel formation. Multiple transcription factors guide angioblasts to differentiate into ECs, essential for vascular development (Olczyk *et al.*, 2023).

In pathological angiogenesis, two main mechanisms occur: sprouting and intussusception. Sprouting angiogenesis involves the dissolution of the basement membrane, allowing ECs to migrate, proliferate, and form new vessel structures (Figure 2.1). Intussusceptive angiogenesis, on the other hand, involves the insertion of cellular columns into existing blood vessels, leading to their growth and remodeling (Deepa K.K., Jannu and Kulambi, 2021; Laschke, Gu and Menger, 2022). These processes are vital for tumour growth and metastasis, as new blood vessels provide tumours with nutrients and a route for metastasis (Zhang *et al.*, 2024).

Anti-angiogenic therapy was proposed as a promising alternative for cancer treatment. This approach aims to disrupt existing blood vessels and inhibit the formation of new vascular networks. As a result, the delivery of oxygen and nutrients to cancer cells is diminished, ultimately slowing tumour growth. For example; specific antibodies, such as bevacizumab, the first VEGF-targeted agent approved by the US FDA for cancer therapy, became available for clinical application (Folkman, 2023).

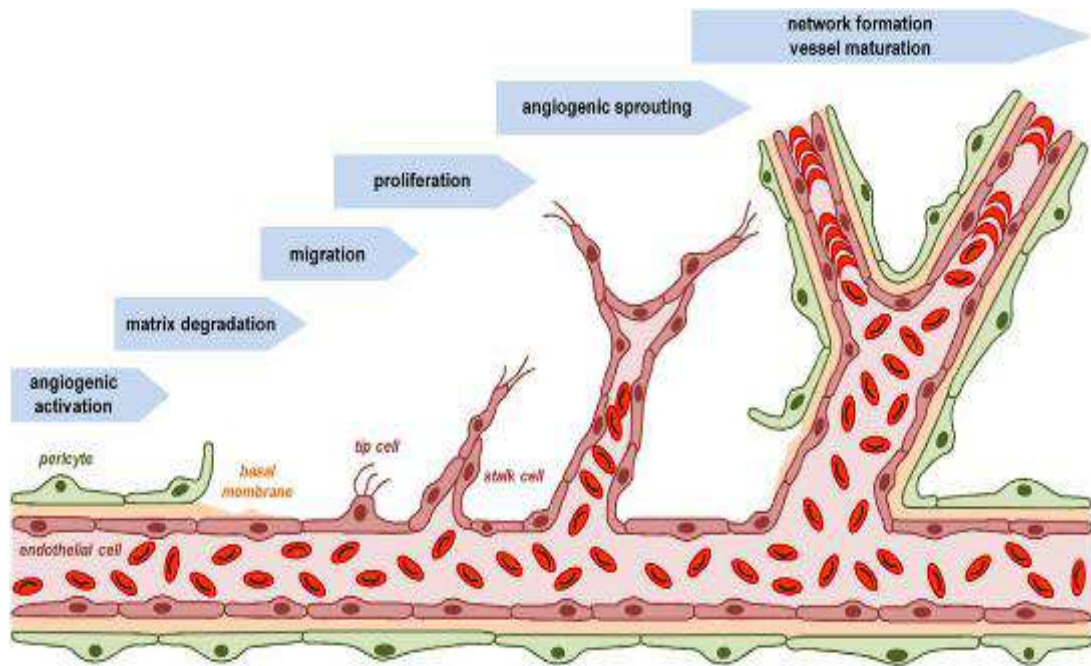


Figure 2.1 The angiogenesis process comprises multiple stages: vessel activation, followed by pericyte detachment, EC migration, and sprout formation that connects to create new microvascular networks supported by a basement membrane (Laschke, Gu and Menger, 2022).

### 2.3.1 The Role of Anti-Angiogenic Therapy in Tumour Development and Metastasis

Anti-angiogenic agents are classified as either direct or indirect. Direct agents specifically target ECs involved in blood vessel formation, inhibiting their proliferation and migration, and are generally independent of cancer cell types, resulting in a low risk of resistance. Indirect agents, on the other hand, block the release of angiogenic factors from tumour tissues, but these agents may face resistance due to the genetic instability of tumour cells. Mixed anti-angiogenic agents, such as protein kinase C inhibitors and multi-targeting kinase inhibitors, aim to concurrently target tumour ECs and malignant cells, enhancing therapeutic efficacy (Haibe *et al.*, 2020).

Angiogenesis is essential for both the early stages of tumour development and the metastatic stage of cancer. As with healthy tissues, tumours need oxygen and

nutrients to thrive, but because they proliferate so quickly, the supply from the existing blood vessels cannot keep up with the demand, as shown in Figure 2.2 (Ayoub *et al.*, 2022). Tumours react by secreting angiogenic substances, like VEGF, which promote the development of new blood vessels that penetrate the tumour and provide a constant flow of oxygen and nutrients. In addition, this new vascular network gives cancer cells a way to access the bloodstream and travel to other areas of the body, which is essential for metastasis (Folkman, 2023).

The angiogenic switch is a crucial process in the early phases of tumour growth that enables microscopic, latent tumours to grow and develop into a state that can be clinically identified. When pro-angiogenic factors, such as matrix metalloproteinases (MMPs), FGF, and VEGF, surpass anti-angiogenic factors, this switch is triggered. In addition to encouraging the creation of blood vessels, these proteins also break down the ECM, which permits endothelial cells to move and create new arteries and fosters the growth of tumours (Dudley and Griffioen, 2023).

Since angiogenesis plays a crucial part in the formation of tumours and their metastasis, anti-angiogenic therapy has become a viable cancer treatment strategy. Patients with metastatic cancer benefit most from anti-angiogenic therapy since angiogenesis is essential for the cancer's progression to distant locations (Ayoub *et al.*, 2022). Tyrosine kinase inhibitors (TKIs) are intended to prevent the creation of blood vessels that enable the growth of primary tumours and the dissemination of tumours to other locations by inhibiting VEGF receptor signaling (Saravanan *et al.*, 2020).

In metastatic colorectal cancer (mCRC), bevacizumab, a monoclonal antibody that binds to VEGF-A selectively, has shown notable efficacy when used in conjunction with chemotherapy. Compared to chemotherapy alone, it has demonstrated better

overall and progression free survival, making it a crucial tool in the treatment of mCRC (Mooi *et al.*, 2021). The overall survival advantages for certain cancer types, including breast, melanoma, pancreatic, and prostate cancers, have been inconsistent, despite the fact that bevacizumab and other anti-angiogenic therapy have been effective in treating metastatic tumours. This variation emphasizes the basic distinctions between various cancer types and how they interact with angiogenic pathways (Olejarz *et al.*, 2020). A combination of treatments that target several pathways involved in both angiogenesis and tumour growth may be necessary due to the complexity of angiogenesis in many malignancies, which can lead to resistance to anti-angiogenic medicines over time. As studies progress, a better comprehension of the molecular processes behind tumour angiogenesis may result in more specialized and successful treatment approaches (Ansari *et al.*, 2022).

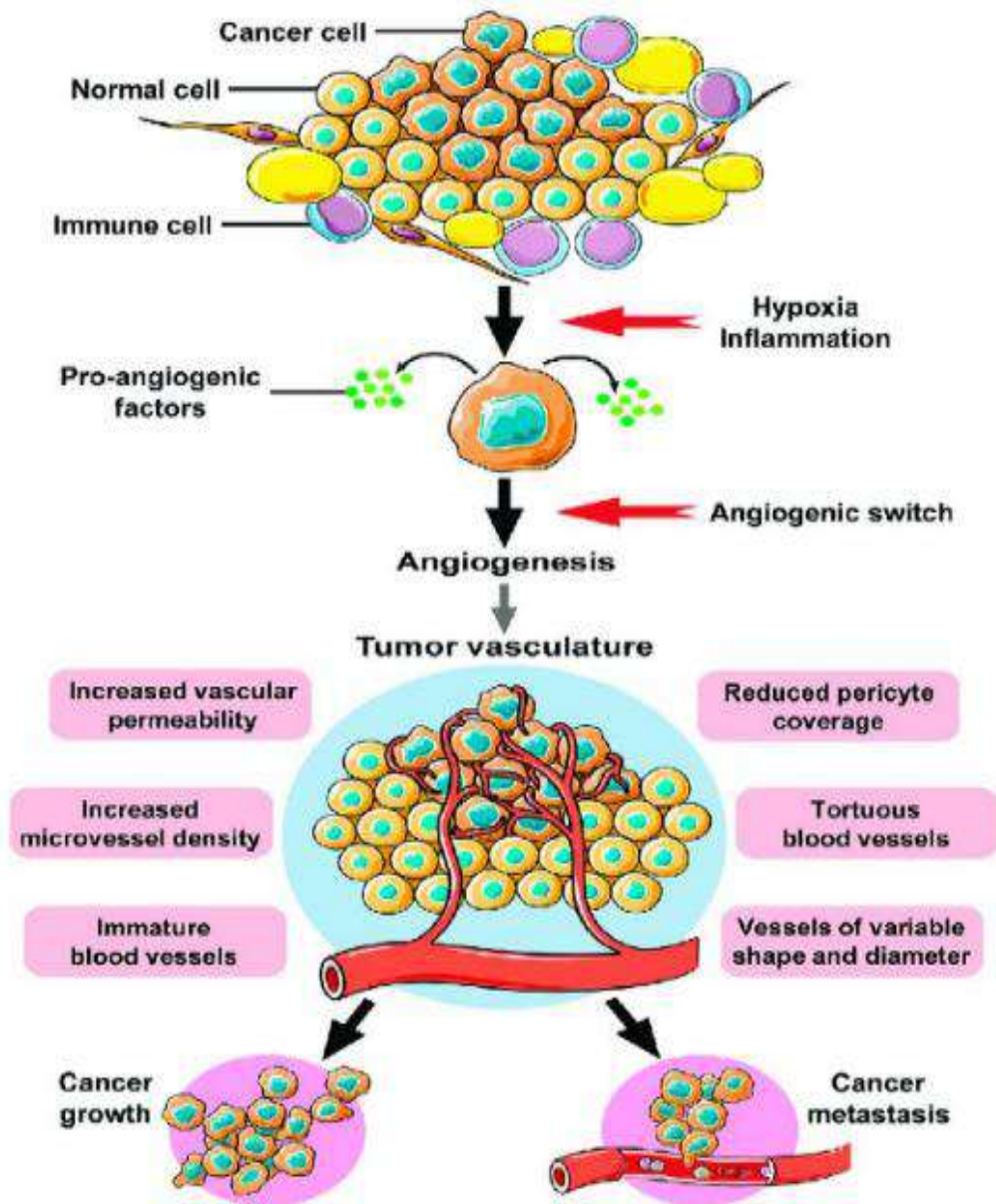


Figure 2.2 Angiogenesis involves the formation of blood vessels, rendering it a critical role in the growth and metastasis of solid cancers. Various factors, such as low oxygen levels, inflammation, and growth signals, can trigger cancer cells to secrete substances that promote the development of blood vessels in tumour cells, consequently aiding their progression (Ayoub et al., 2022).

### **2.3.2 Comprehensive Anti-Angiogenic Therapies and Their Applications in Cancer Treatment**

The overexpression of one or multiple VEGF ligands in tumours of solid origin could be manipulated as an effective anti-angiogenic treatment for various tumour types by blocking the VEGF pathway. Interestingly, the suppression of tumour development in humans has been demonstrated through the suppression of sprouting angiogenesis. Therefore, drugs targeting the VEGF pathway, including sunitinib and bevacizumab, have displayed promising results in specific conditions (Haibe *et al.*, 2020).

In recent years, nanoparticles have developed as a novel approach in anti-angiogenic therapy, offering unique rewards in targeting the tumour microenvironment. Nanoparticles' small size and high surface area-to-volume ratio allow for the direct delivery of anti-angiogenic medicines to the tumour site, increasing therapeutic efficacy while reducing systemic side effects. These nanocarriers can encapsulate various anti-angiogenic agents and facilitate controlled release, allowing for sustained drug levels at the tumour site (de la Torre *et al.*, 2020).

Moreover, nanoparticles can improve the solubility and bioavailability of poorly water-soluble drugs, further enhancing their effectiveness. Studies have shown that certain nanoparticles, such as silver, gold, and polymeric nanoparticles, can inhibit angiogenesis by targeting key pathways involved in the process, including the VEGF signaling pathway. They can also act synergistically with conventional anti-angiogenic agents, enhancing their efficacy against tumour growth and metastasis (Rajora *et al.*, 2020).

Nevertheless, the effectiveness of VEGF signalling inhibition varies across different cancer types, underscoring the need for further assessment to determine the precise targeting of the vasculature in tumours (Olejarz *et al.*, 2020).

### **2.3.2(a) Optimizing Anti-Angiogenic Therapy Through Combination Approaches**

Initial clinical investigations suggested that anti-angiogenic monotherapy for advanced tumours may not be very effective. However, recent trials have shown promise in combining anti-angiogenic agents with chemotherapy. One illustration is the combined use of an anti-VEGF antibody along with chemotherapy as a first-line treatment for mCRC (Kreidieh *et al.*, 2020). Over the past two decades, a range of anti-angiogenic medications targeting the VEGF/VEGFR system has been developed, with some new treatments showing enhanced properties for disrupting VEGF interactions or signaling pathways (Lopes-Coelho *et al.*, 2021).

In addition to VEGF-targeting medications, various anti-angiogenic medicines have also been evaluated in clinical settings as stand-alone treatments or in conjunction with pre-existing therapies. These include kinase inhibitors, COX-2 inhibitors, and Matrix Metalloproteinase Inhibitors (MMPi) (Islam, Jang and Lee, 2024).

Recent developments in nanotechnology have improved these combination treatments even more. Nanoparticles, which act as effective drug delivery vehicles, improve anti-angiogenic drugs' bioavailability and targeting. Encapsulating anti-VEGF antibodies or other anti-angiogenic medications in nanoparticles is feasible to enhance the distribution of these medications to the tumour microenvironment. While reducing systemic toxicity, this strategy improves treatment efficacy (Shen *et al.*, 2022).

Previous study has demonstrated that bevacizumab improves safety profiles and treatment efficacy in clinical trials when paired with chemotherapeutic drugs for a variety of malignancies, such as metastatic renal cancer, non-small cell lung cancer (NSCLC), and late-stage CRC (Nie *et al.*, 2020). The incorporation of nanoparticles in these combination therapies may lead to improved treatment outcomes, including enhanced tumour regression and prolonged survival rates, emphasizing the need for continued research in this promising area (Yang *et al.*, 2021).

### **2.3.2(b) Adjuvant Anti-Angiogenic Strategies in Cancer Management**

Adjuvant anti-angiogenic therapy is used after the initial tumour has been surgically removed in order to prevent tumour recurrence and micrometastatic progression. Clinical trials have contrasted chemotherapy-only treatment versus chemotherapy-bevacizumab treatment in patients with CRC. Overall survival differences between the groups at 3- or 5-year follow-ups were statistically negligible, despite bevacizumab improving progression-free survival. In adjuvant contexts, bevacizumab's effectiveness is still limited, despite its success in treating mCRC (André *et al.*, 2020). Fluorouracil (5-FU) and oxaliplatin, two conventional chemotherapy medications, have shown promise in both adjuvant and metastatic situations. However, despite their success in treating metastatic cases, medications like cetuximab and bevacizumab have not shown comparable outcomes when used as adjuvant therapies for CRC (Zhou *et al.*, 2021).

Significant promise exists for improving therapeutic efficacy by the incorporation of nanoparticles into adjuvant anti-angiogenic treatments. By enhancing the targeted delivery of anti-angiogenic medicines, nanoparticles can minimize systemic negative effects while increasing the concentration of these medications at the